JOC The Journal of Organic Chemistry

Article

pubs.acs.org/joc

Synthesis and Properties of Methoxyphenyl-Substituted Derivatives of Indolo[3,2-b]carbazole

Jurate Simokaitiene,[†] Egle Stanislovaityte,[†] Juozas V. Grazulevicius,*[,†] Vygintas Jankauskas,[‡] Rong Gu,[§] Wim Dehaen,[§] Yi-Chen Hung,[∥] and Chao-Ping Hsu[∥]

[†]Department of Organic Technology, Kaunas University of Technology, Radvilenu pl. 19, LT-50254, Kaunas, Lithuania

[‡]Department of Solid State Electronics, Vilnius University, Sauletekio al. 9, LT-2040, Vilnius, Lithuania

[§]Department of Chemistry, University of Leuven, Celestijnenlaan 200F, B-3001 Leuven, Belgium

[∥]Institute of Chemistry, Academia Sinica, 128 Sec. 2 Academia Road, Taipei 115, Taiwan

Supporting Information

ABSTRACT: The synthesis and full characterization of new derivatives of indolo[3,2-*b*]carbazole with differently substituted phenyl groups at nitrogen atoms is reported. Comparative study on their thermal, optical electrochemical, and photoelectrical properties is presented. The synthesized compounds are electrochemically stable. Their highest occupied molecular orbital energy values range from −5.14 to −5.07 eV. The electron photoemission spectra of the films of synthesized materials revealed the ionization potentials of 5.31−5.47 eV. Hole drift mobility of the amorphous film of 5,11-bis(3-methoxyphenyl)-6-pentyl-5,11-dihydroindolo[3,2-*b*]carbazole exceed 10^{-3} $cm^2/V{\cdot}s$ at high electric fields, as it was established by xerographic time-of-flight technique. In contrast to diphenylamino substituted derivatives of carbazole, no effect of the position of methoxy groups on the photoelectrical properties was observed for the synthesized methoxyphenyl-substituted derivatives of indolo[3,2-*b*]carbazole. The indolo[3,2-*b*]carbazole core has a larger resonance structure that includes 3 phenyl rings, and thus the energy gap of the HOMO and LUMO π orbitals is lower as compared to that of carbazoles. With a larger energy difference between the phenyl substituents and the core moiety, the indolo[3,2-*b*]carbazole derivatives studied all have a weaker coupling between the phenyl group and a much weaker dependence of the molecular properties on the position of substituents on the phenyl groups as compared to those observed in substituted carbazoles.

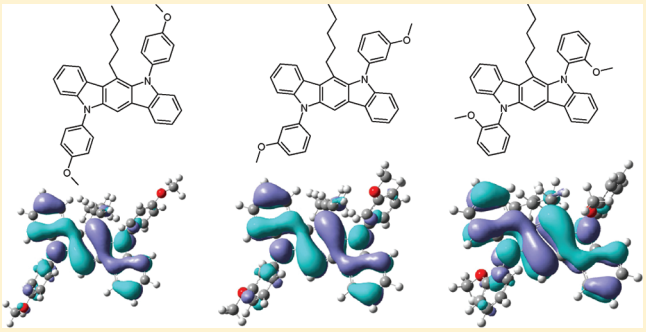

INTRODUCTION

Organic charge-transporting materials are currently widely studied and used as the components of modern electronic and optoelectronic devices such as organic thin film transistors, dye-sensitized and bulk heterojunction solar cells, organic light emitting diodes, electrophotographic photoreceptors.[1−6] Among charge-transporting materials, hole-transporting ones are most widely studied and used. In certain fields of application, e.g., in solid-state dye sensitized solar cells, hole transporting materials with low ionization potentials are required. With the aim of designing organic p-type semiconductors with required set of properties, the structure−properties relationship of aromatic amines was studied. It was established that introduction of methoxy groups into the structures of the derivatives of triphenylamine (TPA) leads to the decrease of their ionization potentials,[7] with stronger influence found in the case of *para*-methoxy substituted TPA compounds as compared to the *meta*-substituted ones.[8] As for the influence of these substitutions on the hole mobilities, lower mobility was observed, for instance, in the case of *p*-methoxy and *p*-butoxy substituted *N*,*N*′-bis(*m*-tolyl)-*N*,*N*′-diphenyl-1,1′-biphenyl-4,4′-diamine (TPD) as compared to the nonsubstituted TPD,[9] which has been partly explained by the change in dipole moment upon substitution. Among organic charge-transporting materials, derivatives of carbazole are also widely synthesized and studied.[10−13] Most of carbazolyl-containing materials are capable of transporting positive charges, i.e., holes; however, recently ambipolar derivatives of carbazole, which are capable of transporting effectively both positive and negative charges, were reported.[14,15] It was recently established that introduction of methoxy-substuted diphenylamino moieties into the structures of carbazole derivatives leads to the decrease of ionization potentials and to the increase of hole drift mobilities.[16] The extent of decrease of ionization potential depends on the position of the methoxy groups. The lowest ionization potentials and the best charge transport properties were observed for the compounds containing one methoxy group in *para*- and *ortho*- positions of phenyl rings of diphenylamino

Received: January 13, 2012
Published: April 26, 2012

Scheme 1

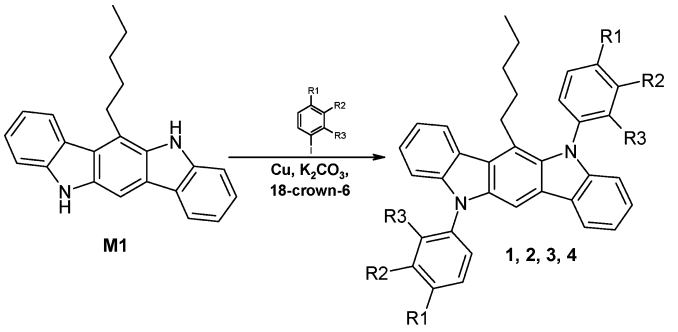

	R1	R2	R3
1	H	H	H
2	-OCH_3	H	H
3	H	-OCH_3	H
4	H	H	-OCH_3

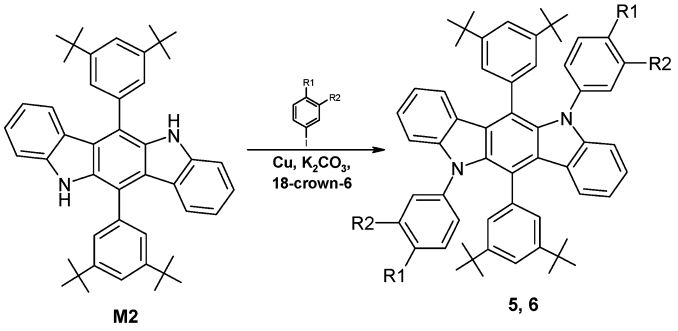

	R1	R2
5	-OCH_3	H
6	H	-OCH_3

moiety. Indolocarbazoles represent a class of very promising but until now much less studied of organic semiconductors. Substituted indolo[3,2-*b*]carbazoles were successfully used for the preparation of high-mobility organic thin film transistors.[17−21] The best performance was observed for vapor deposited thin films of 3,9-diphenyl-5,11-dioctylindolo[3,2-*b*]carbazole[19] and 3,9-di(*p*-octylbenzene)-5,11-dihydroxyindolo[3,2-*b*]carbazole[20] with the maximum field-effect mobility of 0.22 $cm^2\ V^{-1}\ s^{-1}$. Derivatives of indolo[3,2-*b*]carbazole are also regarded as promising materials for efficient electroluminescence.[22] In addition, indolo[3,2-*b*]-carbazole copolymers were reported as potential photovoltaic materials.[23,24] They can also be applied in anion complexation and sensing.[25] To our knowledge, the influence of methoxy groups on the properties of the derivatives of indolo[3,2-b]carbazole has not yet been studied.

In this article, we report on the synthesis and properties of new derivatives of indolo[3,2-*b*]carbazole containing differently substituted phenyl groups at 5 and 11 positions. The aims of this work were to extend the choice of charge-transporting derivatives of indolo[3,2-*b*]carbazole and to study the influence of phenyl moieties having methoxy groups in the different positions on the properties of the materials.

RESULTS AND DISCUSSION

Methoxyphenyl-substuted derivatives of 5,11-dihydroindolo-[3,2-*b*]carbazole (**2**−**6**) were synthesized as described in Scheme 1 from 6-pentyl-5,11-dihydroindolo[3,2-*b*]carbazole (**M1**) or 6,12-di(3,5-di-*tert*-butylphenyl)-5,11-dihydroindolo-[3,2-*b*]carbazole (**M2**) and the corresponding iodoanisoles by Ullmann coupling.[26] 6-Pentyl-5,11-dihydroindolo[3,2-*b*]-carbazole (**M1**)[27,28] and 6,12-di(3,5-di-*tert*-butylphenyl)-5,11-dihydroindolo[3,2-*b*]carbazole (**M2**)[29] were prepared by the earlier reported procedures. 5,11-Bisphenyl-6-pentyl-5,11-dihydroindolo[3,2-*b*]carbazole (**1**) was prepared for the comparison of the properties by the similar synthetic route.[29] All the compounds (**1**−**6**) were purified by column chromatography. They were identified by elemental analysis, IR, ^{1}H NMR, ^{13}C NMR, and mass spectrometries.

The behavior on heating of compounds **1**−**6** was studied by DSC and TGA under a nitrogen atmosphere. The values of glass transition temperatures (T_g), melting points (T_m), crystallization temperatures (T_{cr}), and the temperatures of the onsets of thermal degradation (T_{ID}) are summarized in Table 1.

Table 1. Thermal Characteristics of Compounds 1−6

compound	T_m, °C	T_{cr}, °C	T_g, °C	T_{ID}, °C
1	185		55	422
2	230	176	65	441
3	157		57	432
4	199		76	426
5	371	271		453
6	364	309		469

The synthesized compounds demonstrate high thermal stability. The values of T_{ID} well exceed 400 °C, as confirmed by TGA with a heating rate of 20 °C/min. The derivatives of 6,12-di(3,5-di-*tert*-butylphenyl)-5,11-dihydroindolo[3,2-*b*]-carbazole (**5**, **6**) having extended aromatic system show superior thermal stability relative to that of the derivatives of 6-pentyl-5,11-dihydroindolo[3,2-*b*]carbazole (**1**−**4**).

Compounds **1**−**6** were isolated after the synthesis as crystalline materials. In the first DSC heating scans, they showed endothermal melting signals with the maxima in the range of 157−364 °C. Compounds **1**−**4** can exist in the solid amorphous phase; i.e., they form molecular glasses. Their glass transition temperatures (T_g) range from 46 to 76 °C. The morphological stability of the molecular glass of **2** seems to be somewhat lower than that of **1**, **3**, and **4**. In the second DSC heating scan, it shows not only glass transition at 65 °C but also crystallization at 176 °C with the following melting at 230 °C (Figure 1b). Compounds **1**, **3**, and **4** showed the comparable behavior in the DSC experiments. As an example, DSC curves

dx.doi.org/10.1021/jo202677j | J. Org. Chem. 2012, 77, 4924−4931

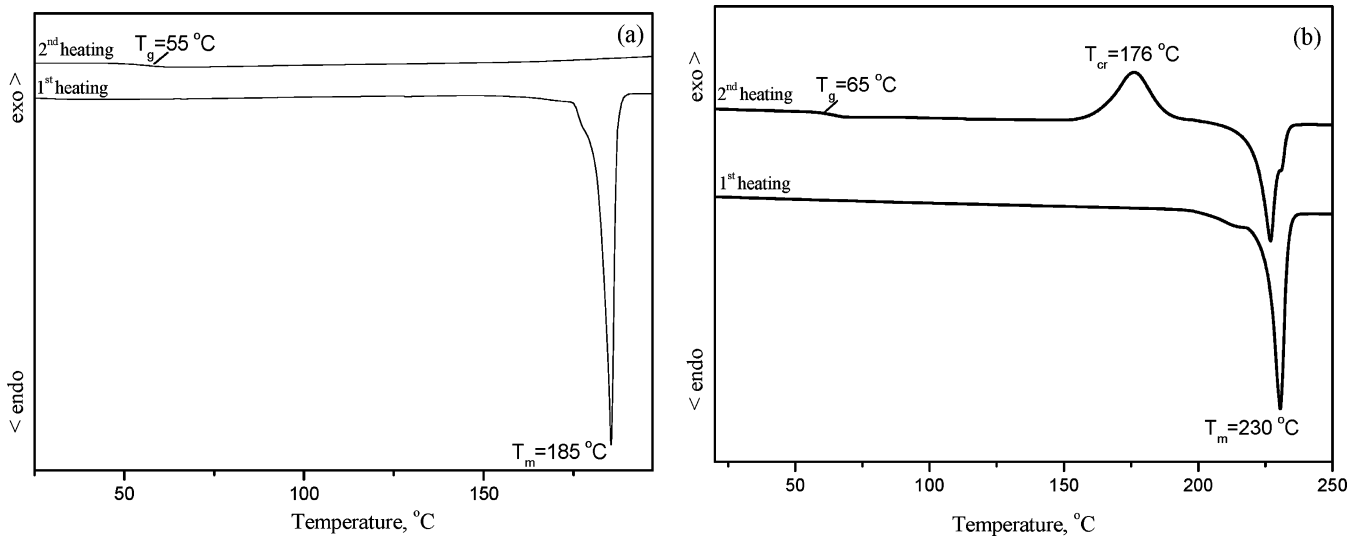

Figure 1. DSC termograms of compounds **1** (a) and **2** (b) (scan rate 10 °C/min, N_2 atmosphere).

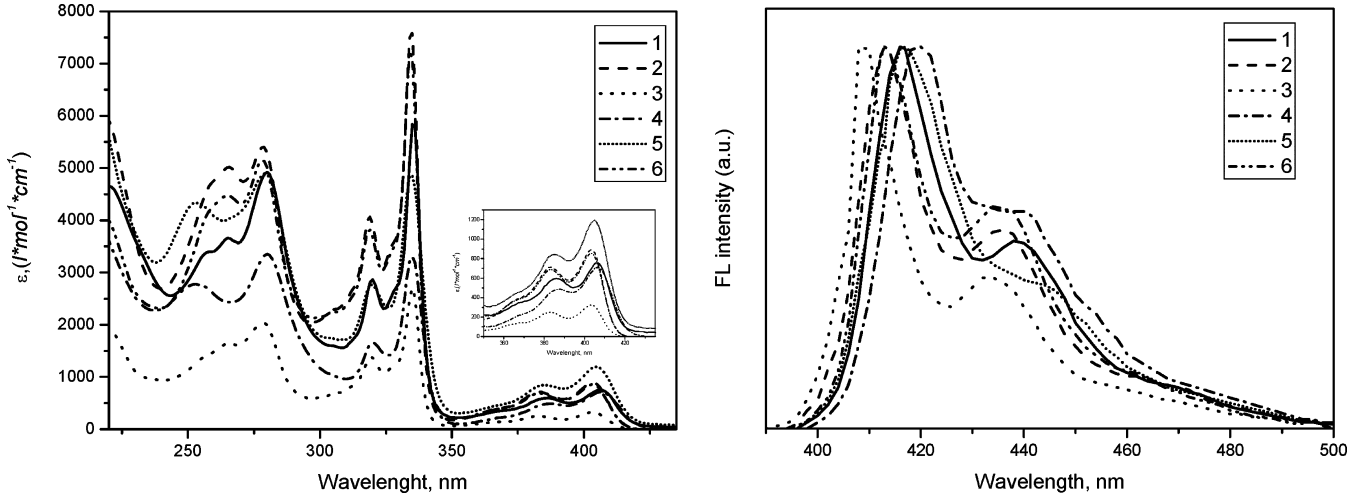

Figure 2. UV and fluorescence spectra of dilute THF solutions (10^{-5} mol/L) of compounds **1**–**6**.

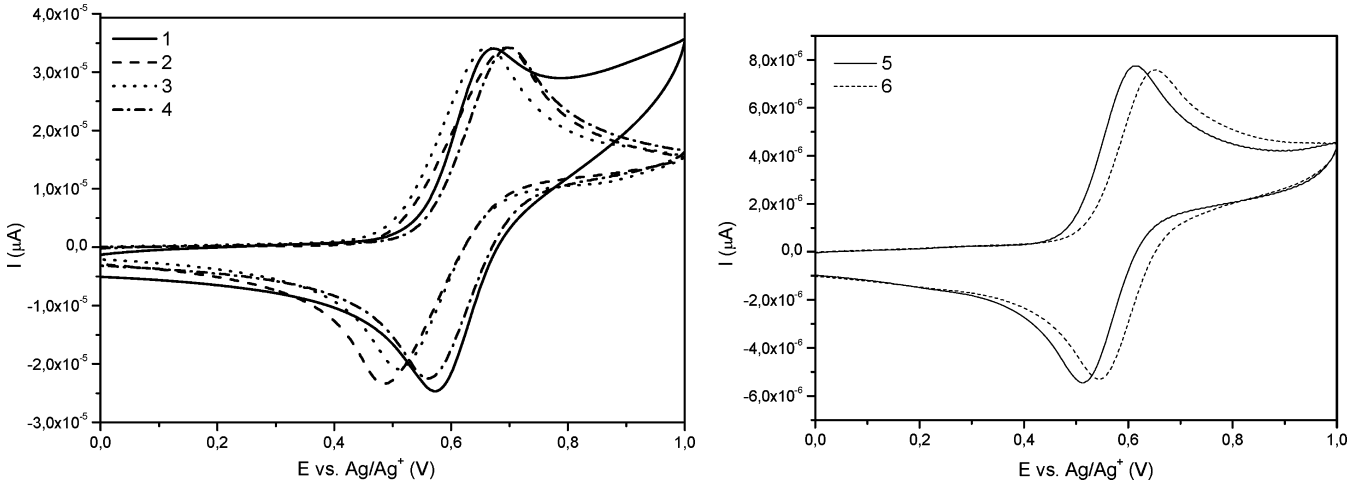

Figure 3. Cyclic voltammograms of compounds **1**–**6** in dichloromethane at 25 °C at sweep rate of 0.1 V/s.

of compound **1** are shown in Figure 1a. In the first heating scan, compound **1** showed melting at 185 °C. Upon cooling, it did not crystallize and showed glass transition at 55 °C in the second heating scan. Comparison of T_g of compound **1** with those of compounds **2**–**4** shows that introduction of methoxy groups leads to the increase of T_g. The highest T_g is observed

dx.doi.org/10.1021/jo202677j | J. Org. Chem. 2012, 77, 4924–4931

for compound **4**, having methoxy groups in *ortho* positions. Apparently, methoxy groups situated close to the nitrogen atoms hinder rotation of phenyl rings around C−N bonds. Compounds **5** and **6** could not be transformed into the glassy state by cooling from the melt.

Figure 2 shows UV and fluorescence spectra of dilute solutions of compounds **1**−**6**. UV and fluorescence spectra of compounds **1**−**6** are similar to those of indolo[3,2-*b*]-carbazole.[30] Absorption edges and low-energy absorption maxima of 4-methoxyphenyl-substituted compounds **2** and **5** exhibit small bathochromic shifts with respect to those of 2- or 3-methoxyphenyl-substituted compounds (**3**, **4**, **6**). Fluorescence spectrometry data correlate with the UV spectrometry results. Fluorescence spectra are similar to those of alkyl-substituted indolo[3,2-*b*]carbazole.[31] The fluorescence intensity maxima of **2** and **5** are slightly red-shifted with respect of those of **3**, **4**, and **6.**

To elucidate the energetic conditions for energy and electron transfer in dilute solutions, the HOMO/LUMO energy values were estimated by cyclic voltammetry (CV). The cyclic voltammograms of the synthesized compounds in dichloromethane show a quasi-reversible oxidation couple (Figure 3). The electrochemical data are summarized in Table 2. The

Table 2. HOMO, LUMO, Band Gap Energies, Ionization Potentials, and Electrochemical Characteristics[a] of Compounds 1−6

compound	$E_{1/2}$ vs Fc/V	E_g^{opt}/eV[b]	I_p/eV[c]	E_{HOMO}/eV[d]	E_{LUMO}/eV[e]
1	0.33	2.99	5.39	−5.13	−2.14
2	0.30	2.95	5.31	−5.10	−2.15
3	0.34	2.98	5.41	−5.14	−2.16
4	0.30	2.99	5.35	−5.10	−2.11
5	0.27	2.95	5.47	−5.07	−2.12
6	0.30	2.94	5.47	−5.10	−2.16

[a]The measurements were carried out at a glassy carbon electrode in dichloromethane solutions containing 0.1 M tetrabutylammonium perchlorate as electrolyte and $Ag/AgNO_3$ as the reference electrode. Each measurement was calibrated with Fc. [b]The optical band gaps E_g^{opt} estimated from the edges of electronic absorption spectra. [c]Ionization energy E_{Ip} was measured by the photoemission in air method from films. [d]$E_{HOMO} = 4.8 + E_{1/2}$ vs Fc. [e]$E_{LUMO} = E_{HOMO} - E_g^{opt}$

oxidation potentials for reversible oxidation were taken as the average of the anodic and cathodic peak potentials. The E_{HOMO} values were determined from the first oxidation potential values with respect to ferrocene (Fc). The E_{HOMO} values of the synthesized compounds are very close and range from −5.14 to −5.07 eV. The E_{LUMO} levels were determined from optical energy band gaps and E_{HOMO} values. They are also close and range from −2.16 to −2.11 eV.

The ionization potentials (I_p) of amorphous layers of compounds **1**−**6** established by electron photoemission method in air range from 5.31 to 5.47 eV (Table 2). The ionization potentials recorded for the derivatives of 6-pentyl-5,11-dihydroindolo[3,2-*b*]carbazole (**1**−**4**) are a little lower than those observed for the derivatives of 6,12-di(3,5-di-*tert*-butylphenyl)-5,11-dihydroindolo[3,2-*b*]carbazole (**5**, **6**). The lowest ionization potential is observed for 4-methoxyphenyl-substituted compound **2**. Nevertheless, in contrast to our earlier observation,[21] the influence of the position of methoxy groups on the values of ionization potential is not very obvious for these series of materials. The differencies observed in the values of HOMO and I_p energy levels obtained by electron photoemission spectrometry and by electrochemical studies can be explained by the differencies in molecular interactions and molecular arrangements in thin solid layers and in dilute solutions.

In order to obtain insights on the electronic properties of the molecules studied, quantum chemical calculations were performed. The core model indolo[3,2-*b*]carbazole molecules, **M1** and **M2**, were also included in the computational study. Two different theoretical estimates for the vertical ionization potential (I_p) energies are listed in Table 3, with first being the

Table 3. *Ip*, Excitation Energies, Population Analysis Data, and Dihedral Angles (°) for Molecules 1−6 and the Core Models M1 and M2

	I_p, eV[a]		excitation energies, eV[b]			
molecule	HF-KT	ΔDFT	TDDFT	CIS	substituent charge[c]	dihedral angles[d]
1	6.91	6.00	3.33	4.72	0.226	56; 59
2	6.83	5.83	3.30	4.71	0.242	64; 64
3	6.84	5.87	3.33	4.72	0.229	60; 60
4	6.66	5.79	3.35	4.71	0.216	64; 65
5	6.71	5.73	3.36	4.69	0.174	90; 80
6	6.69	5.72	3.36	4.70	0.171	93; 93
M1	6.82	6.23	3.36	4.71		
M2	6.71	5.95	3.36	4.70		

[a]Vertical ionization potential reported. Both are calculated with 6-31G* basis set. The B3LYP functional is employed in ΔDFT. [b]Vertical excitation energies reported for the S_1 state. The B3LYP functional is employed in TDDFT, and the 6-31G* basis set is used for both data sets. [c]The amount of additional positive charge on the two methoxyphenyl groups upon ionization. [d]The dihedral angles between the phenyl groups and the indolo[3,2-*b*]carbazole core, in degrees. For molecules **1**−**4**, the first numbers refer to the one without steric interaction with the pentyl substituent.

negative energy of the HOMO from a HF calculation following the Koopmans theorem (HF-KT), and the second is the difference of the DFT total energies of the neutral or cationic molecules (ΔDFT). All calculations were performed with a developmental version of Q-Chem.[32]

From Table 3, it is seen that all I_p values obtained are very similar across all molecules studied, for both I_p data sets. The I_p values and the excitation energies of the core model molecules (**M1** and **M2**) are similar to those of the substituted molecules. For the similar I_p values, we analyzed the electron population in ionization. As shown in Figure 4, all the HOMO are concentrated in the core region, with a small population in the amine and the methoxyphenyl-substituents. On the other hand, the excitation is also pretty much localized to the core region, as seen in the natural transition orbital (NTO) plots included in Figure 4. The NTOs are a set of 1-electron orbitals that best describe the electron hole in a transition. They are equivalent to the HOMO and LUMO if the S_1 state were a pure transition from HOMO to LUMO, and NTOs are more general, as they can include the effects of other MOs if they are also involved.[33] It is seen that both ionization and the excitation are mainly in the indolo[3,2-*b*]carbazole core.

We have also performed the population analysis on the difference charge of the cationic and the neutral states, to gain a quantitative picture on the distribution of the charge. The data given in Table 3 show that ca. 17−24% of the positive charge is

dx.doi.org/10.1021/jo202677j | J. Org. Chem. 2012, 77, 4924−4931

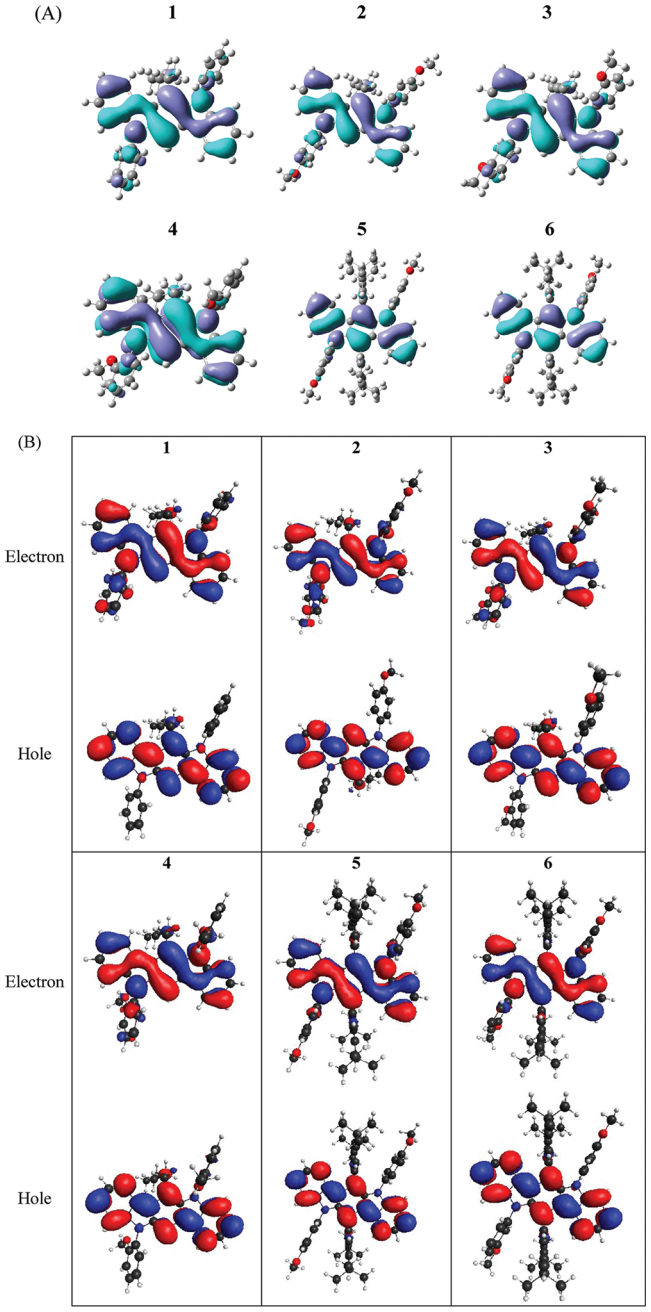

Figure 4. (A) HOMOs and (B) NTOs of molecules **1**–**6**. The HOMOs are models for the ionized electrons, while the NTOs are the electron and hole orbitals involved in an excitation. In all cases, the population of the NTOs shown constitutes more than 94% of the excited states. Contour surfaces at the isovalue of 0.02 au are shown.

distributed to the two methoxyphenyl groups. The dihedral angles between the phenyl substituents and the core indolo[3,2-*b*]carbazole, derived from DFT computational structures, are also listed in Table 3. It is seen that they are quite large, ranging from 56 to 93 degrees, which limits the electronic interaction between those moieties. For molecules **1**–**4**, the two dihedral angles are similar, and the nearby pentyl groups do not affect the angle much. We note that the pentyl group is likely offering an attractive CH–π interaction, instead of a bulky, repulsive interaction (Figure S1 in the Supporting Information). From these results, we conclude that the electronic structure of molecules **1**–**6** is very similar to those of their indolo[3,2-*b*]carbazole cores, and the methoxyphenyl substituents have rather small effect on the I_p and the excitation energy values.

In an earlier work,[16] the methoxyphenyl substituents were attached to an amino group, which was attached to the carbon at the third position of a carbazole ring, and the dihedral angles between the carbazole and the methoxy phenylene were between 35 and 58 degrees for DFT structures. The HOMO for those molecules were shown to be delocalized to the methoxyphenyl-substituents, and the position of methoxy substituent in the phenyl group had a more significant effect than for our current set of molecules. The phenyl amine group in the substituents contributed to the delocalization of HOMO, and the HOMO energy would be higher. On the other hand, the indolo[3,2-*b*]carbazole core has a larger resonance structure that includes 3 phenyl rings, and thus the energy gap between the HOMO and LUMO is smaller as compared to that of carbazoles. We have calculated the HOMO and LUMO energies for the fragment models, benzene, methoxybenzene, carbazole, and indolo[3,2-*b*]carbazole. As seen in Table 4,

Table 4. HOMO and LUMO Energies and the Corresponding Energy Gap, in the Units of eV[a]

molecule	HOMO	LUMO	gap
benzene	−6.70	0.10	6.80
methoxybenzene	−6.44	0.01	6.45
indolo[3,2-b]carbazole	−4.92	−1.00	3.92
N-phenyl indolo[3,2-b]carbazole	−4.88	−1.01	3.87
carbazole	−5.44	−0.64	4.80
N-phenyl carbazole	−5.33	−0.65	4.68

[a]Obtained with the B3LYP functional and 6-31G* basis set. While DFT may not offer the right energies for the HOMO and LUMO, and the energy gaps prediction is rather limited, we note that these results are mainly used for discussion on the origin of localized HOMO and LUMO distribution within a set of calculation.

indolo[3,2-*b*]carbazole has a larger energy difference with the phenyl substituents (benzene or methoxybenzene) in both HOMO and LUMO, as compared to that of carbazole. For indolo[3,2-*b*]carbazole, the larger energy differences in HOMO (LUMO) between the phenyl group and the core group leads to a smaller perturbative interaction, and thus a smaller contribution from the phenyl group in the HOMO (LUMO) indolo[3,2-*b*]carbazole. As a result, the HOMO (LUMO) energies for the *N*-phenyl carbazole and *N*-phenyl indolo[3,2-*b*]carbazole are very similar to those of the core carbazoles. The smaller contribution can also explain the much weaker dependence of the molecular properties on the position of substituents on the phenyl groups as compared to those in substituted carbazoles.

The I_p values of the core molecules (**M1** and **M2**) are in general higher than those of the substituted molecules. The addition of di-*tert*-butylphenyl groups to the indolo[3,2-*b*]carbazole core slightly reduces the I_p. The position of the methoxy groups in molecules **2**–**4** slightly affects the I_p energy. Molecules **2** and **4** have slightly lower I_p, which should have to do with their *ortho* and *para* substitution that allows a resonance in the electrons. However, this effect is very small because of the low coupling between the methoxyphenyl group and the indolo[3,2-*b*]carbazole core, and this effect is barely observable in experimental data (Table 2). On the other hand, the dihedral angles for molecules **5** and **6** are even larger than

dx.doi.org/10.1021/jo202677j | J. Org. Chem. 2012, 77, 4924–4931

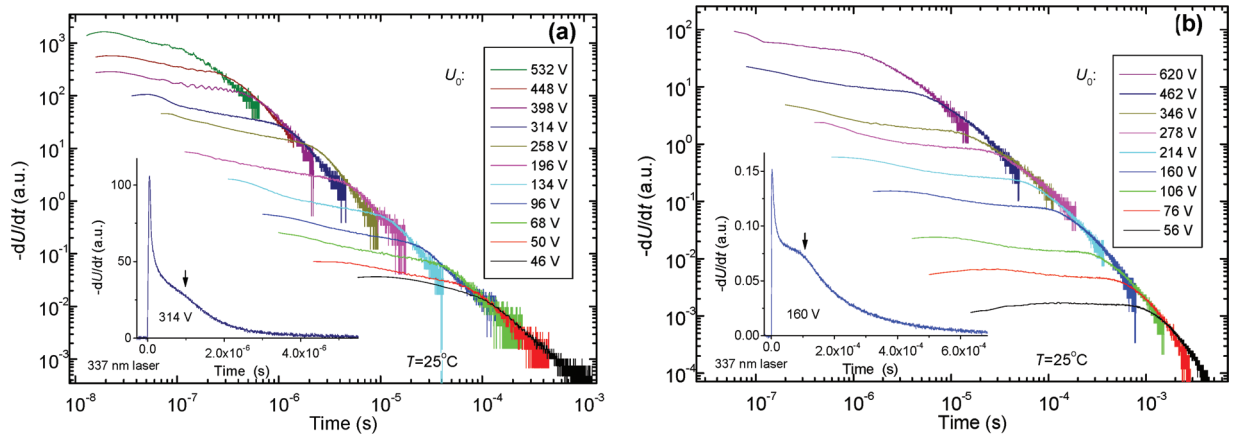

Figure 5. XTOF transients of the neat film of compound **3** (a) and of the layer of compound **3** doped in PC-Z (50%) (b).

for other molecules, likely because of the presence of bulky di-*tert*-butyl phenyl substituents. Molecules **5** and **6** are very similar in their physical properties, and the values of I_p and excitation energies are very close to that of the core model **M2**.

Time of flight measurements were used to characterize charge-transporting properties of the synthesized compounds. The representative *dU*/*dt* transients for the neat film of compound **3** and for the solid solution of **3** in PC-Z are shown in Figure 5. Distinct inflection points indicating transit times with the sign of nondispersive hole transport were observed in air both for the neat film of **3** and for its molecular mixture with PC-Z. Nondispersive hole transport was also observed for the glassy layer of compound **4**. The layers of compound **1** and of molecular mixtures of compounds **1**, **2**, **4**–**6** with PC-Z exhibited dispersive charge transport. These differences in charge transport can apparently be explained by the differences in molecular packing.

Figure 6 shows electric field dependencies of hole drift mobilities (μ) for the amorphous layers of compounds **1**, **3**, **4**

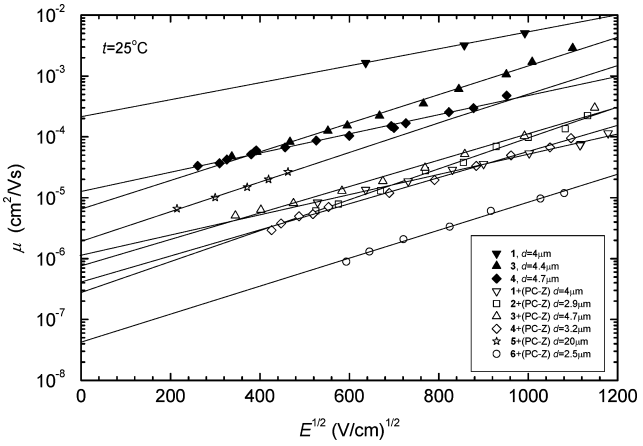

Figure 6. Electric field dependencies of hole drift mobility in charge transport layers of compounds **1**, **3**, **4** and compounds **1**–**6** doped in PC-Z (50%).

and for the bisphenol Z polycarbonate molecularly doped with compounds **1**–**6**. At room temperature, μ showed linear dependencies on the square root of the electric field for all the samples studied. The hole-drift mobility values are summarized in Table 5.

Table 5. Hole Mobility Data for the Amorphous Layers of Net Compound 1, 3, 4 and Compounds 1–6 Doped in PC-Z (50%)

charge-transporting material	μ_0[a], cm²/V·s	μ[b], [cm²/V·s]
1	2.1×10^{-4}	2.8×10^{-3}
3	7×10^{-6}	5×10^{-4}
4	1.3×10^{-5}	2.3×10^{-4}
1+(PC-Z), 1:1	1.2×10^{-6}	2.4×10^{-5}
2+(PC-Z), 1:1	3×10^{-7}	3×10^{-5}
3+(PC-Z), 1:1	8×10^{-7}	4×10^{-5}
4+(PC-Z), 1:1	4×10^{-7}	2.1×10^{-5}
5+(PC-Z), 1:1	1.9×10^{-6}	1.8×10^{-5} [c]
6+(PC-Z), 1:1	4.4×10^{-8}	3×10^{-6}

[a]The zero field hole drift mobility. [b]The hole drift mobility at electric field of 6.4×10^5 V/cm. [c]The hole drift mobility at electric field of 1.6×10^5 V/cm.

Among the layers of the net materials, the best charge-transporting properties were observed for compound **1** having no methoxy groups. Hole drift mobilities in the layers of **1** well exceed of 10^{-3} cm²/V·s at high electric fields. No clear effect of the position of methoxy groups on charge-transporting properties can be identified for this series of materials. Among methoxy-substituted derivatives of 6-pentyl-5,11-dihydroindolo[3,2-b]carbazole (**2**–**4**), the best charge transport properties were observed for compound **3** having methoxy groups in *meta* positions. The glassy layer of compounds **3** showed hole drift mobility of 5×10^{-4} cm²/V·s at an electric field of 6.4×10^5 V/cm at room temperature. Compound **3** also showed the best performance in the molecular mixture with bisphenol Z poycarbonate The 50% solid solution of **3** in PC-Z demonstrated hole drift mobility of 4×10^{-5} cm²/V·s at the electric field of 6.4×10^5 V/cm. Among the derivatives of 6,12-di(3,5-di-*tert*-butylphenyl)-5,11-dihydroindolo[3,2-*b*]carbazole (**5**, **6**), the superior charge-transporting properties were shown by compound **5** having methoxy groups in *para* positions. The molecular mixture of **5** with PC-Z showed hole mobilities of 1.8×10^{-5} cm²/V·s at the electric field of 1.6×10^5 V/cm.

■ CONCLUSIONS

In conclusion, we have synthesized new derivatives of indolo[3,2-*b*]carbazole with phenyl groups having methoxy groups in different positions. The synthesized compounds exhibit high thermal stability with the temperatures of the onset of thermal degradation ranging from 426 to 469 °C. The

dx.doi.org/10.1021/jo202677j | J. Org. Chem. 2012, 77, 4924–4931

derivatives of 6-pentyl-5,11-dihydroindolo[3,2-*b*]carbazole form glasses with glass transition temperatures of 46−76 °C. The HOMO values of the synthesized compounds range from −5.14 to −5.07 eV. The electron photoemission spectra of the films of the materials revealed ionization potentials of 5.31−5.47 eV. The lowest ionization potential was observed for 4-methoxyphenyl-substituted compound, i.e., for 5,11-bis(4-methoxyphenyl)-6-pentyl-5,11-dihydroindolo[3,2-*b*]carbazole. Time-of-flight hole drift mobilities of the amorphous films of 5,11-bis(3-methoxyphenyl)-6-pentyl-5,11-dihydroindolo[3,2-*b*]carbazole exceed 10^{-3} $cm^2/V{\cdot}s$ at high electric fields. The indolo[3,2-*b*]carbazole core has a larger resonance structure that includes 3 phenyl rings, and thus the energy difference of the HOMO and LUMO π orbitals is lower as compared to that of carbazoles. The energy difference between the phenyl substituents and the core moiety becomes larger. The lower energy in the core moiety of indolo[3,2-*b*]carbazoles leads to a larger energy gap between the phenyl substituents and the core moiety, and therefore, the indolo[3,2-*b*]carbazole derivatives studied all have a weaker coupling between the phenyl group and a much weaker dependence of the molecular properties on the position of substituents on the phenyl groups as compared to those observed in substituted carbazoles.

EXPERIMENTAL SECTION

General Procedure. Compounds **2**−**6** were prepared by the method of Ullmann and Bielecki.[22] The reaction mixtures consisting of 6-pentyl-5,11-dihydroindolo[3,2-*b*]carbazole (**M1**) (1.00 g, 3.06 mmol) or 6,12-di(3,5-di-*tert*-butylphenyl)-5,11-dihydroindolo[3,2-*b*]-carbazole (**M2**) (1.94 g, 3.06 mmol), potassium carbonate (2.88 g, 20.81 mmol), iodoanisole (2.86 g, 12.24 mmol), copper (0.78 g, 12.24 mmol), 18-crown-6 (0.16 g, 0.61 mmol), and 1,2-dichlorobenzene (ca. 8 mL) were stirred at reflux temperature for 24 h. The reaction mixtures were cooled down and filtrated, the solvent was distilled in a vacuum, and the crude product was subjected to silica gel column chromatography.

5,11-Bis(4-methoxyphenyl)-6-pentyl-5,11-dihydroindolo-[3,2-*b*]carbazole (2). Prepared according to the general procedure from 6-pentyl-5,11-dihydroindolo[3,2-*b*]carbazole (**M1**) and 4-iodoanisole. The resulting solid product was purified by column chromotography using an eluent mixture of chloroform and hexane in a volume ratio of 1:4. Yellowish crystals were obtained with a yield of 1.1 g (67%); mp = 226−228 °C.

^{1}H NMR (300 MHz, $CDCl_3$, δ, ppm): 0.86 (t, 3H, J = 7 Hz), 1.05−1.30 (m, 4H), 1.48−1.72 (m, 2H), 3.00−3.13 (m, 2H), 3.92 (s, 3H), 3.93 (s, 3H), 6.92 (d, 1H, J = 8 Hz), 7.07 (d, 2H, J = 9 Hz), 7.11−7.37 (m, 7H), 7.43 (d, 2H, J = 9 Hz), 7.52 (d, 2H, J = 9 Hz), 7.81 (s, 1H), 8.04 (d, 1H, J = 8 Hz), 8.13 (d, 1H, J = 8 Hz).

^{13}C NMR (75.4 MHz, $CDCl_3$, δ, ppm): 14.5, 22.8, 28.6, 29.4, 32.7, 55.9, 55.9, 97.5, 109.5, 110.2, 115.0, 115.5, 119.2, 119.3, 120.1, 121.6, 121.8, 122.9, 123.3, 123.7, 124.5, 125.4, 126.1, 129.5, 130.9, 131.1, 134.0, 135.8, 138.2, 143.0, 145.4, 159.2, 159.8.

IR, ν_{max} (KBr), 3050 (CH_{Ar}), 2952, 2910 ($CH_{aliph.}$), 2861, 2836 (CH_3−O-), 1610, 1515, 1462, 1452 (C═C_{Ar}), 1319 (C−N); γ cm^{-1}: 742 (CH_{Ar}).

MS calcd for $C_{37}H_{34}N_2O_2$ 538.70, (APCI+, 20 V), m/z: 539 ([M + H]$^+$).

5,11-Bis(3-methoxyphenyl)-6-pentyl-5,11-dihydroindolo-[3,2-*b*]carbazole (3). Prepared according to the general procedure from 6-pentyl-5,11-dihydroindolo[3,2-*b*]carbazole (**M1**) and 3-iodoanisole. The resulting solid product was purified by column chromotography using an eluent mixture of chloroform and hexane in a volume ratio of 1:4. White crystals were obtained with a yield of 1.2 g (73%); mp = 154−156 °C.

^{1}H NMR (300 MHz, $CDCl_3$, δ, ppm): 0.85 (t, 3H, J = 7 Hz), 1.05−1.30 (m, 4H), 1.48−1.78 (m, 2H), 3.00−3.15 (m, 2H), 3.82 (s, 3H), 3.88 (s, 3H), 6.99 (d, 1H, J = 8 Hz), 7.03−7.60 (m, 13H), 7.95 (s, 1H), 8.07 (d, 1H, J = 8 Hz), 8.14 (d, 1H, J = 8 Hz).

^{13}C NMR (75.4 MHz, $CDCl_3$, δ, ppm): 14.5, 22.8, 28.7, 29.4, 32.7, 55.7, 55.8, 97.8, 109.7, 110.4, 113.6, 114.7, 115.0, 119.5, 119.7, 120.2, 120.3, 121.8, 122.1, 123.0, 123.5, 123.9, 124.7, 125.5, 126.3, 130.5, 131.0, 135.8, 137.7, 139.6, 142.5, 142.6, 145.0, 160.9, 161.2.

IR, ν_{max} (KBr), 3047 (CH_{Ar}), 2957, 2917 ($CH_{aliph.}$), 2854 (CH_3−O−), 1599, 1491, 1467, 1455 (C═C_{Ar}), 1316 (C−N); γ cm^{-1}: 748 (CH_{Ar}).

MS calcd for $C_{37}H_{34}N_2O_2$ 538.70, (APCI+, 20 V), m/z: 539 ([M + H]$^+$).

5,11-Bis(2-methoxyphenyl)-6-pentyl-5,11-dihydroindolo-[3,2-*b*]carbazole (4). Prepared according to the general procedure from 6-pentyl-5,11-dihydroindolo[3,2-*b*]carbazole (**M1**) and 2-iodoanisole. The resulting solid product was purified by column chromotography using a mixture of chloroform and hexane in a volume ratio of 1:4 as the eluent. Yellowish crystals were obtained with a yield of 0.74 g (45%); mp = 195−196 °C.

^{1}H NMR (300 MHz, $CDCl_3$, δ, ppm): 0.85 (t, 3H, J = 7 Hz), 1.00−1.28 (m, 4H), 1.48−1.74 (m, 2H), 2.90−3.22 (m, 2H), 3.65 (s, 3H), 3.70 (d, 3H, J = 3 Hz), 6.84 (d, 1H, J = 8 Hz), 7.08−7.38 (m, 9H), 7.45−7.57 (m, 4H), 7.66 (s, 1H), 8.03 (d, 1H, J = 7 Hz), 8.12 (d, 1H, J = 7 Hz).

^{13}C NMR (75.4 MHz, $CDCl_3$, δ, ppm): 14.5, 22.9, 28.5, 29.5, 32.8, 55.8, 56.1, 97.9, 109.9, 112.3, 113.2, 113.2, 118.9, 119.1, 120.0, 121.2, 121.4, 121.6, 121.9, 122.7, 123.5, 123.8, 124.5, 125.1, 125.9, 126.7, 129.6 129.7, 130.2, 131.8, 135.4, 137.8, 142.7, 144.4, 156.7, 157.7.

IR, ν_{max} (KBr), 3049 (CH_{Ar}), 2957, 2929 ($CH_{aliph.}$), 2871, 2837 (CH_3−O-), 1596, 1500, 1464 (C═C_{Ar}), 1321 (C−N); γ cm^{-1}: 741 (CH_{Ar}).

MS calcd for $C_{37}H_{34}N_2O_2$ 538.70, (APCI+, 20 V), m/z: 539 ([M + H]$^+$).

5,11-Bis(4-methoxyphenyl)-6,12-di(3,5-di-*tert*-butylphenyl)-5,11-dihydroindolo[3,2-*b*]carbazole (5). Prepared according to the general procedure from 6,12-di(3,5-di-*tert*-butylphenyl)-5,11-dihydroindolo[3,2-*b*]carbazole (**M2**) and 4-iodoanisole. The resulting solid product was purified by column chromotography using an eluent mixture of chloroform and hexane in a volume ratio of 1:2. Yellowish crystals were obtained with a yield of 0.9 g (67%); mp = 350−352 °C.

^{1}H NMR (300 MHz, $CDCl_3$, δ, ppm): 1.29 (s, 36H), 3.74 (s, 6H), 6.51 (s, 1H), 6.53 (s, 1H), 6.58 (d, 4H, J = 8 Hz), 6.74−6.81 (m, 4H), 6.90 (d, 4H, J = 8 Hz), 7.02 (d, 4H, J = 2 Hz), 7.13−7.23 (m, 2H), 7.29 (t, 2H, J = 2 Hz).

^{13}C NMR (75.4 MHz, $CDCl_3$, δ, ppm): 31.7, 35.1, 55.4, 109.8, 114.0, 118.7, 120.1, 121.0, 122.7, 123.2, 123.4, 125.1, 125.4, 130.9, 132.1, 134.5, 136.6, 145.0, 150.4, 158.1.

IR, ν_{max} (KBr), 3048 (CH_{Ar}), 2963 ($CH_{aliph.}$), 2865 (CH_3−O-), 1595, 1510, 1456 (C═C_{Ar}), 1389, 1362 (*tert*-butyl), 1314 (C−N); γ cm^{-1}: 745 (CH_{Ar}).

MS calcd for $C_{60}H_{64}N_2O_2$ 845.19, (APCI+, 20 V), m/z: 845 ([M + H]$^+$).

5,11-Bis(3-methoxyphenyl)-6,12-di(3,5-di-*tert*-butylphenyl)-5,11-dihydroindolo[3,2-*b*]carbazole (6). Prepared according to the general procedure from 6,12-di(3,5-di-*tert*-butylphenyl)-5,11-dihydroindolo[3,2-*b*]carbazole (**M2**) and 3-iodoanisole. The resulting solid product was purified by column chromotography using a mixture of chloroform and hexane in a volume ratio of 1:2 as an eluent. Yellowish crystals were obtained with a yield of 0.9 g (67%); mp = 362−363 °C.

^{1}H NMR (300 MHz, $CDCl_3$, δ, ppm): 1.26 (s, 18H), 1.29 (s, 18H), 3.67 (s, 6H), 6.55 (s, 1H), 6.57 (s, 1H), 6.60−6.65 (m, 2H), 6.68−6.82 (m, 6H), 6.97 (t, 4H, J = 8 Hz), 7.12−7.24 (m, 6H), 7.28 (t, 2H, J = 2 Hz).

^{13}C NMR (75.4 MHz, $CDCl_3$, δ, ppm): 31.8, 31.7, 35.0, 35.1, 55.3, 109.9, 112.8, 115.5, 118.9, 120.3, 121.1, 122.6, 122.8, 123.4, 123.5, 124.8, 125.1, 125.5, 129.4, 134.5, 136.4, 140.5, 144.7, 150.3, 150.6, 159.6.

IR, ν_{max} (KBr), 3049 (CH_{Ar}), 2961 ($CH_{aliph.}$), 2867 (CH_3−O-), 1591, 1491, 1459 (C═C_{Ar}), 1386, 1362 (*tert*-butyl), 1317 (C−N); γ cm^{-1}: 743 (CH_{Ar}).

dx.doi.org/10.1021/jo202677j | *J. Org. Chem.* 2012, 77, 4924−4931

MS calcd for $C_{60}H_{64}N_2O_2$ 845.19, (APCI+, 20 V), m/z: 845 ($[M + H]^+$).

■ ASSOCIATED CONTENT

Supporting Information

General experimental conditions, ^1H and ^{13}C NMR spectra for all new compounds, and the details of quantum chemical calculations. This material is available free of charge via the Internet at http://pubs.acs.org.

■ AUTHOR INFORMATION

Corresponding Author

*E-mail: juozas.grazulevicius@ktu.lt.

Notes

The authors declare no competing financial interest.

■ ACKNOWLEDGMENTS

This research was funded by a grant (No. MIP-059/2011) from the Research Council of Lithuania. W.D. thanks the F. W. O.-Vlaanderen, the Ministerie voor Wetenschapsbeleid, and the University of Leuven for continuing financial support.

■ REFERENCES

(1) Shirota, Y.; Kageyama, H. *Chem. Rev.* **2007**, *107*, 953−1010.
(2) Pron, A.; Gawrys, P.; Zagorska, M.; Djuradoa, D.; Demadrillea, R. *Chem. Soc. Rev.* **2010**, *39*, 2577−2632.
(3) Boudreault, P. L. T.; Najari, A.; Leclerc, M. *Chem. Mater.* **2011**, *23*, 456−469.
(4) Huang, J.; Su, J. H.; Li, X.; Lam, M. K.; Fung, K. M.; Fan, H. H.; Cheah, K. W.; Chen, C. H.; Tian, H. *J. Mater. Chem.* **2011**, *21*, 2957−2964.
(5) Jung, B. J.; Tremblay, N. J.; Yeh, M. L.; Katz, H. E. *Chem. Mater.* **2011**, *23*, 568−582.
(6) Facchetti, A. *Chem. Mater.* **2011**, *23*, 733−758.
(7) Seo, E. T.; Nelson, R. F.; Fritsch, J. M.; Marcoux, L. S.; Leedy, D. W.; Adams, R. N. *J. Am. Chem. Soc.* **1966**, *88*, 3498.
(8) Pan, J. H.; Chou, Y. M.; Chiu, H. L.; Wang, B. C. *Aust. J. Chem.* **2009**, *62*, 483−492.
(9) Maldonado, J. L.; Bishop, M.; Fuentes-Hernandez, C.; Caron, P.; Domercq, B.; Zhang, Y. D.; Barlow, S.; Thayumanavan, S.; Malagoli, M.; Bredas, J. L.; Marder, S. R.; Kippelen, B. *Chem. Mater.* **2003**, *15*, 994−999.
(10) Grazulevicius, J. V.; Strohriegl, P.; Pielichowski, J.; Pielichowski, K. *Prog. Polym. Sci.* **2003**, *28*, 1297−1353.
(11) Xie, J. T.; Ning, Z. J.; Tian, H. *J. Photochem. Photobiol., A* **2003**, *154*, 169−177.
(12) Li, J.; Grimsdale, A. C. *Chem. Soc. Rev.* **2010**, *39*, 2399−2410.
(13) Boudreault, P. L. T.; Beaupre, S.; Leclerc, M. *Polym. Chem.* **2010**, *1*, 127−136.
(14) Shen, J. Y.; Yang, X. L.; Huang, T. H.; Lin, J. T.; Ke, T. H.; Chen, L. Y.; Wu, C. C.; Yeh, M. C. P. *Adv. Funct. Mater.* **2007**, *17*, 983−995.
(15) Tomkeviciene, A.; Grazulevicius, J. V.; Kazlauskas, K.; Gruodis, A.; Jusenas, S.; Ke, T. H.; Wu, C. C. *J. Phys. Chem. C* **2011**, *15*, 4887−4897.
(16) Sakalyte, A.; Simonaitiene, J.; Tomkeviciene, A.; Keruckas, J.; Buika, G.; Grazulevicius, J. V.; Jankauskas, V.; Hsu, C. P.; Yang, C. H. *J. Phys. Chem. C* **2011**, *115*, 4856−4862.
(17) Li, Y.; Wu, Y.; Gardner, S.; Ong, B. S. *Adv. Mater.* **2005**, *17*, 849−853.
(18) Wakim, S.; Bpouchard, J.; Simard, M.; Drolet, N.; Tao, Y.; Leclerc, M. *Chem. Mater.* **2004**, *16*, 4386−4388.
(19) Boudreault, P. L.; Wakim, S.; Blouin, N.; Simard, M.; Tessier, C.; Tao, Y.; Leclerc, M. *J. Am. Chem. Soc.* **2007**, *129*, 9125−9136.
(20) Boudreault, P. L.; Wakim, S.; Tang, M. L.; Tao, Y.; Bao, Z.; Leclerc, M. *J. Mater. Chem.* **2009**, *19*, 2921−2928.
(21) Boudreault, P. L.; Virkar, A. A.; Bao, Z.; Leclerc, M. *Org. Electron.* **2010**, *11*, 1649−1659.
(22) Zhao, H. P.; Wang, F. Z.; Yuan, C. X.; Tao, X. T.; Sun, J. L.; Zou, D. C.; Jiang, M. H. *Org. Electron.* **2009**, *10*, 925−931.
(23) Wakim, S.; Aich, B. R.; Tao, Y.; Leclerc, M. *Polym. Rev.* **2008**, *48*, 432−462.
(24) Zhou, E.; Yamakawa, S.; Zhang, Y.; Tajima, K.; Yang, C.; Hasimoto, K. *J. Mater. Chem.* **2009**, *19*, 7730−7737.
(25) Gale, P. A. *Chem. Commun.* **2008**, 4525−4540.
(26) Ullmann, F.; Bielecki, J. *Chem. Ber.* **1901**, *34*, 2174−2178.
(27) Gu, R.; Hameurlaine, A.; Dehaen, W. *Synlett* **2006**, *10*, 1535−1538.
(28) Tang, C.; Liu, F.; Xia, Y. J.; Xie, L. H.; Wei, A.; Li, S. B.; Fan, Q. L.; Huang, W. *J. Mater. Chem.* **2006**, *16*, 4074−4080.
(29) Gu, R.; Van Snick, S.; Robeyns, K.; Van Meervelt, L.; Dehaen, W. *Org. Biomol. Chem.* **2009**, *7*, 380−385.
(30) Kirkus, M.; Grazulevicius, J. V.; Grigalevicius, S.; Gu, R.; Dehaen, W.; Jankauskas, V. *Eur. Polym. J.* **2009**, *45*, 410−417.
(31) Belletete, M.; Blouin, N.; Boudreault, P. L. T.; Leclerc, M.; Durocher, G. *J. Phys. Chem. A* **2006**, *110*, 13696−13704.
(32) Shao, Y.; Molnar, L. F.; Jung, Y.; Kussmann, J.; Ochsenfeld, C.; Brown, S. T.; Gilbert, A. T. B.; Slipchenko, L. V.; Levchenko, S. V.; O'Neill, D. P., Jr.; Distasio, R. A.; Lochan, R. C.; Wang, T.; Beran, G. J. O.; Besley, N. A.; Herbert, J. M.; Lin, C. Y.; Van Voorhis, T.; Chien, S. H.; Sodt, A.; Steele, R. P.; Rassolov, V. A.; Maslen, P. E.; Korambath, P. P.; Adamson, R. D.; Austin, B.; Baker, J.; Bird, E. F. C.; Dachsel, H.; Doerksen, R. J.; Drew, A.; Dunietz, B. D.; Dutoi, A. D.; Furlani, T. R.; Gwaltney, S. R.; Heyden, A.; Hirata, S.; Hsu, C. P.; Kedziora, G.; Khalliulin, R. Z.; Klunziger, P.; Lee, A. M.; Lee, M. S.; Liang, W. Z.; Lotan, I.; Nair, N.; Peters, B.; Proynov, E. I.; Pieniazek, P. A.; Rhee, Y. M.; Ritchie, J.; Rosta, E.; Sherrill, C. D.; Simmonett, A. C.; Subotnik, J. E.; Woodcock, H. L., III.; Zhang, W.; Bell, A. T.; Chakraborty, A. K.; Chipman, D. M.; Keil, F. J.; Warshel, A.; Herhe, W. J.; Schaefer, H. F., III.; Kong, J.; Krylov, A. I.; Gill, P. M. W.; Head-Gordon, M. *Phys. Chem. Chem. Phys.* **2006**, *8*, 3172−3191.
(33) Martin, R. *J. Chem. Phys.* **2006**, *118*, 4775.